Power Budget Analysis for High Altitude Airships

Sang H. Choi, James R. Elliott, and Glen C. King
NASA Langley Research Center
Hampton, Virginia 23681-2199

The High Altitude Airship (HAA) has various potential applications and mission scenarios that require onboard energy harvesting and power distribution systems. The energy source considered for the HAA's power budget is solar photon energy that allows the use of either photovoltaic (PV) cells or advanced thermoelectric (ATE) converters. Both PV cells and an ATE system utilizing high performance thermoelectric materials were briefly compared to identify the advantages of ATE for HAA applications in this study. The ATE can generate a higher quantity of harvested energy than PV cells by utilizing the cascaded efficiency of a three-staged ATE in a tandem mode configuration. Assuming that each stage of ATE material has the figure of merit of 5, the cascaded efficiency of a three-staged ATE system approaches the overall conversion efficiency greater than 60%. Based on this estimated efficiency, the configuration of a HAA and the power utility modules are defined.

I. Introduction

The applications and uses of high-altitude airships (HAA) extensively cover sensing, probing, surveying, and monitoring and may include surveillance for Homeland Security, earth observing for science and weather monitoring, etc. Commercial applications include monitoring and controlling the ever-increasing complexities of aerial and maritime transportation and telecommunication networks. Such HAA application scenarios require a substantial amount of power to operate surveillance systems, probes, sensors, telescopes, radar, directed high energy devices, etc.. This significant level of power for the envisioned roles of the HAA requires onboard power generation or energy harvesting and storage systems. The propulsion and maneuverability required for transit and stabilization of the HAA at these altitudes also necessitate a significant amount of power. The size and weight of HAA are determined by the requirements of on-station performance and long-term operation. Accordingly, there is little room for incorporation of fuel-carrying power generators which limit the operational time or otherwise increase the overall weight. The power technology for HAA maneuverability and mission-oriented applications must come from its surroundings, e.g. solar power. Conventional photovoltaic cells have been used for NASA's long duration airplanes, the solar-powered Pathfinder, and remotely piloted aircraft [1]. Accordingly, solar power can be regarded as one of the power sources for airships. There are several energy conversion technologies for solar energy. Among them is the photovoltaic (PV) cell array which has been widely used for satellite power sources. However, the cost and weight of high efficiency photovoltaic cells pose a number of shortcomings for wide acceptance and unlimited applications. Other options include the fuel cell, but it is a fuel-carrying power generation system. A conceptual study for the HAA power budget plan has been done at NASA Langley Research Center by utilizing new nanomaterials for solar power harvesting.

II. Advanced Thermo-Electric (ATE) Energy Conversion System

II-1. ATE Material Design

In the past, NASA developed and has used thermoelectric energy conversion systems for the satellites that have missions for deep space exploration. The thermal energy source was radioisotope materials, such as Polonium-210 and Curium-242, which generate thermal energy close to 140 Watts/gram when they radioactively decay.

The energy harvesting system considered in this analysis for the HAA is based on advanced thermoelectric (TE) materials that are currently being developed at NASA Langley Research Center for a targeted Figure of Merit (FoM) goal greater than 5 (see Figure 1). As indicated in Figure 1, the FoM for most TE materials developed so far is still below 2 [2]. A FoM of 1 is approximately equivalent to the thermal conversion efficiency greater than 6 %.

To develop such advanced TE materials with a high FoM, a new material design was invented by a group at NASA Langley Research Center [3-7] to increase the electrical conductivity (EC) and simultaneously reduce the thermal conductivity (TC) by incorporating nano structures [7,8] specially tailored for phonon blocking into TE materials. Within a crystalline structure of a material, the heat transfer mechanism is mainly dictated by phonon transmission (> 70%) rather than by energetic electrons (< 30%) at temperatures below 900 K [9]. Accordingly, a method to manipulate the phonon transmission within a crystalline medium will offer a capability to control the thermal conductivity. The nanostructures populating the bulk matrix TE materials essentially create large phonon scattering cross-sections that effectively block the transfer of thermal energy through them. The TE material in an unoccupied area that is sandwiched between nanostructures will become a phonon bottleneck since the narrowly sandwiched bulk material is under a high tension by the formation of material-rich boundary around the nanostructures. The structure of the material boundary surface around the nanostructures may be framed of a high energy bonding group that develops high tension over the surface. The material structure with high tension would be less subjected to an oscillatory mode transmission than material structures in normal tension. Therefore, both the high tension and the narrow passage between nanostructures are resistive to phonon transmission and accordingly regarded as a phonon bottleneck. Ultimately, the imbedded nanostructures create the phonon scattering cross-sections and bottlenecks throughout the matrix material.

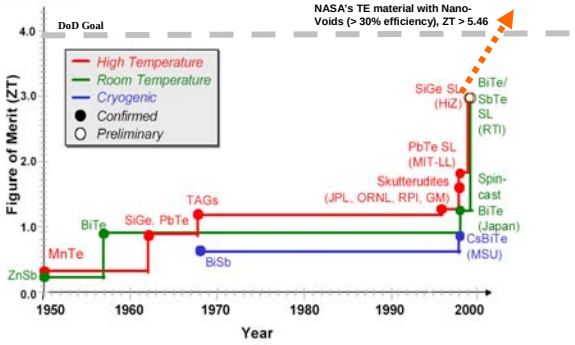

Figure 1. History of Thermoelectric Figure of Merit, ZT. [2]

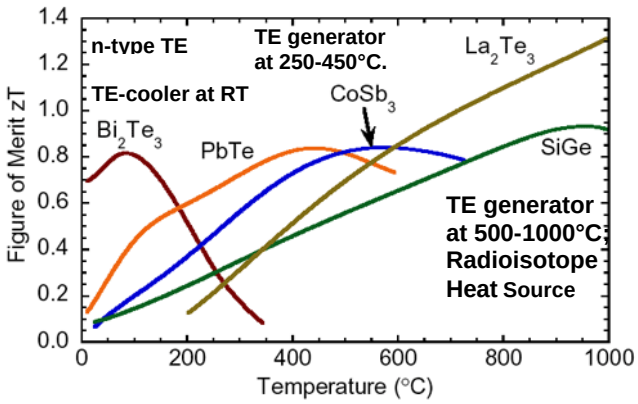

Figure 2. Figure of merit variation of TE materials based on temperature [10].

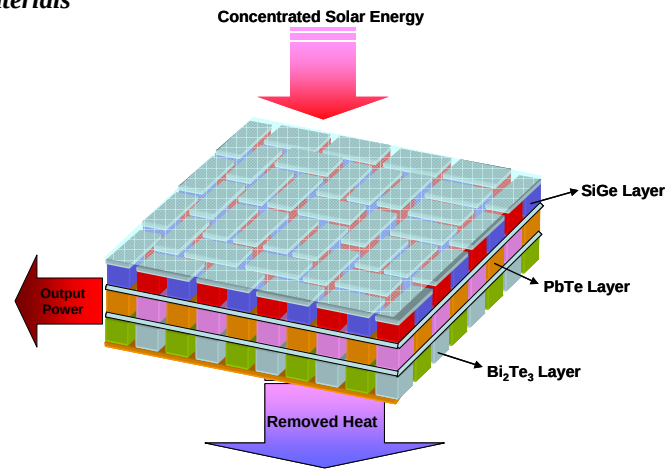

Figure 3. Configuration of ATE device for solar energy conversion

The materials selected for ATE are silicon-germanium (SiGe) and bismuth telluride (Bi_2Te_3). Material selection was based on according to the temperature range where the performance of the TE materials is suitably optimized. In practice, the skills gained from successful development of such an ATE material can be readily extended to the fabrication of other materials, including cobalt antimonide ($CoSb_3$) and lead telluride ($PbTe_3$), which operate best at different temperature ranges. Figure 2 shows several TE materials [10] along with most-suitable use temperature ranges. There are several methods to imbed nanostructures into a matrix material. Silicon germanium requires its own lattice-matched layer for high charge mobility. After a lattice-matched thin-film layer is developed, a layer of nanostructure array is placed on top of the lattice-matched SiGe thin-film layer. Repeating the process above forms a multiple-layered structure of lattice-matched SiGe thin-film layer and void

structure array. On the other hand, the process required for bismuth telluride TE material is quite different from that of SiGe. By the solvo-thermal method, nanocrystals of bismuth telluride are created and then mixed with artificially tailored nanostructures before solvent casting. Through solvent casting on a substrate after mixing, a cake of bismuth telluride is made. This cake goes through calcination and hydrogen plasma etching processes to remove unwanted impurity elements. Finally, the sponge form of bismuth telluride is sintered and then develops a crystalline structure by forming lattice bridges between nanocrystals. After sintering and forming lattice development, the material structure of bismuth telluride resembles to a matrix of single crystal deposition process [5,6].

II-2. Design of ATE Devices

To make a p-n junction for TE energy conversion, the TE matrix materials developed undergo doping processes to create an n-type and a p-type. An array of a pair of p-n junction materials is necessary to increase the thermal exposure area. The ATE energy conversion device consists of triple layers of p-n- junction arrays in a tandem mode as shown in Figure 3. The first layer is built from the array of SiGe while the second and third layers are respectively built from PbTe and Bi_2Te_3 as regenerative cycles. Such an arrangement allows effective energy harvesting from a heat source. For a specific HAA energy harvesting application, the solar energy is considered as an energy source. First, solar flux is concentrated and heats up the first layer which is built with high temperature SiGe. The unused thermal energy from the first layer is subsequently used by the second layer which is built with mid temperature PbTe. Again, the third layer of Bi_2Te_3 uses the unused energy from the second layer to maximize the conversion of the energy that is otherwise rejected. In this fashion, the ATE devices become more effective than solar cells because the performance of solar cells is monolithically tied to the band-gap energy structure, so that they only couple within certain spectral lines. Also the higher the efficiency of solar cells is, the higher the cost and complexity of fabrication. Figure 4 shows a depiction of TE conversion efficiency goals and is added onto an existing diagram of solar cell efficiencies (shown for comparison). Compared to solar cell technology in efficiency, the ATE is competitive. However, considering the available energy from solar flux, the ATE, using thermal energy, can harness more broadband energy than photovoltaic cells which are only band structured to capture photons that are resonant with the discrete, allowed transition energies between the valence and conduction bands of the material. At this junction after the theoretical estimation, the development of a prototype ATE system is underway at NASA Langley Research Center. Although the process of ATE material development seems to be a very difficult and complex challenge as the history of TE material development indicated in Figures 1 and 4, the NASA's new TE material design with imbedded nanostructure may offer a clue to achieve high figure of merit. It is especially worthy to explore the potential benefits because of broad applications, such as energy harvesting and solid-state cooling.

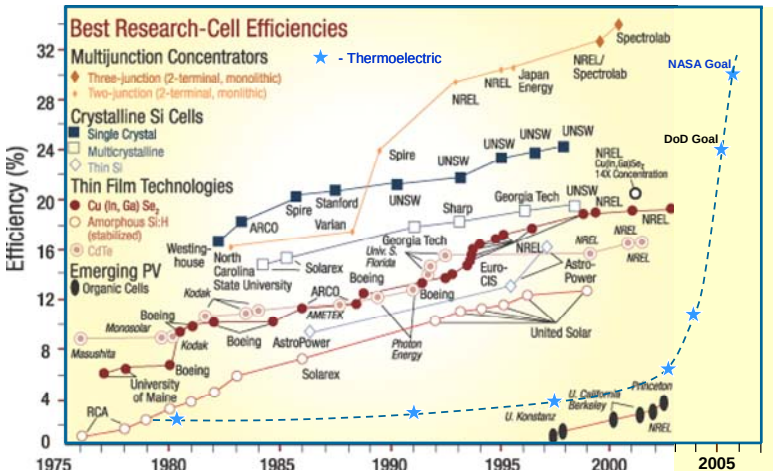

Figure 4. Efficiencies of State-of-the-Art Solar & Thermoelectric Cells.

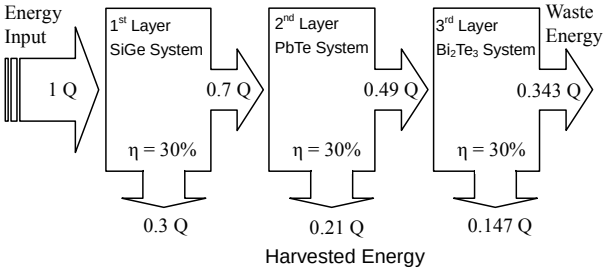

Figure 5. Cascaded efficiency of 3-layer ATE systems in a tandem mode.

II-3. Cascaded Efficiency

There are several potential candidate energy harvesting technologies for high altitude airships, such as solar cells [11], fuel cells [11], Sterling engines, and TE generators. Among them, the advanced TE materials appeared to be attractive for this study because of the cascaded efficiency of multi-layer TE modules that are much higher than the efficiency of a single layer and the broad spectrum of solar thermal energy. The layered structure of the advanced TE materials is specifically engineered to provide maximum efficiency for the corresponding range of operational temperatures. For three layers of the advanced TE materials that operate at high, medium, and low temperatures, correspondingly in a tandem mode, the cascaded efficiency is estimated to be greater than 60 % as indicated in Figure 5. Such a highly effective energy harvesting feature of tandem system [12] based on the three layers of advanced TE materials, which are under development at NASA Langley Research Center, is regarded as the basis of the HAA power budget plan.

II-4. Power Harvesting at Daytime

To maximize the reception of solar thermal energy, the ellipsoid cross-sectioned HAA with a 150 meters long, 60 meters wide, and 24 meters high configuration as shown in Figure 6 is considered. In size, the HAA is about 2.5 times larger than a Goodyear blimp which is 60 meters long. With these HAA dimensions, the normal incident solar power amounts to about 9 MW. However, the daytime exposure varies with sun location. If it is necessary, the HAA can be reoriented to receive the maximum solar energy by keeping the top surface of HAA always perpendicular to the solar angle. When the top surface of HAA follows the sun, the Power Management and Control (PMC) station installed under the belly of HAA is designed to move on a guide rail to reposition itself, always dangling at the bottom of HAA for every collector orientation. Figure 7 shows the repositioned PMC at the nadir point of HAA along with the sun position. In such a manner, the energy harvested from sunrise to sunset becomes relatively even over the day exposure variation. Using 20% efficient photovoltaic (PV) cells, the maximum converted power would be less than 2 MW. With the advanced TE materials of the same efficiency, the converted power would be greater than 4 MW because the cascaded efficiency of three layers is calculated to be approximately 49%. Considering a three-layered structure of the advanced TE materials with the FOM 5, the cascaded efficiency amounts to be close to 66 % (see Figure 5). If the total amount of losses, 35%, due to geometrical orientation (23%), reflection (7%), absorption (3%), and transmittance (2%) is considered for estimation of the cascaded efficiency, the total harvestable unit becomes 0.427 under this 0.65Q input condition instead of the 1Q used in Figure 5. Accordingly, the obtainable power is 3.84 MW which is a substantial amount for several envisioned HAA roles. Figure 6 depicts some of the scenarios that might be feasible, such as a mother ship to wirelessly feed power to deployed unmanned vehicles for atmospheric science missions and telecommunication purposes.

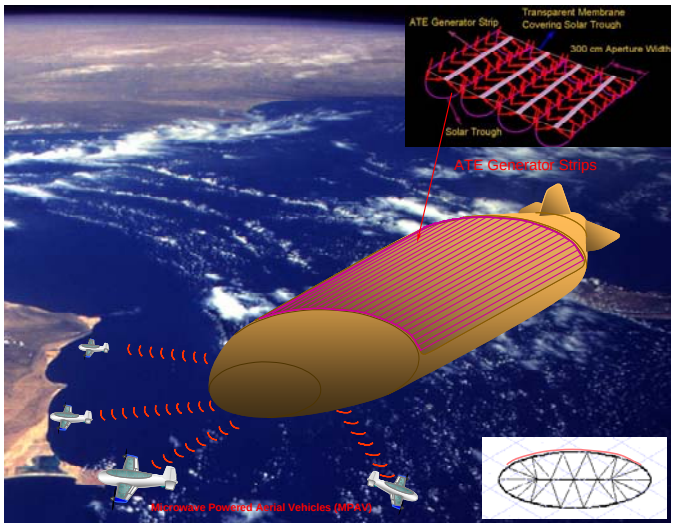

Figure 6. HAA model with ellipsoidal cross-section to maximize reception of the solar flux.

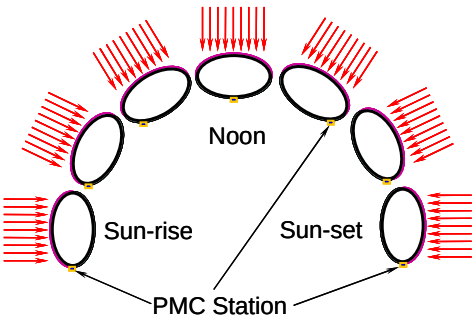

Figure 7. Reorientation of HAA along the sun position. The power management and control (PMC) station moves on a guide rail to position itself always at the nadir point of the HAA.

The ATE power module uses linear parabolic troughs with 30 cm aperture width to collect solar power as shown in Figure 8. The back-surface of ATE strips is reflective to reduce solar energy absorption and faces outside directly to the cold, high altitude environment to drop the surface temperature by convective cooling. The temperature at 70,000 feet or above in the atmosphere is extremely cold and hovers below – 73°C [13]. Accordingly, to maximize the performance of ATE, the solar trough concentrators are used to focus solar flux to the 1st layer that faces the reflector while the back side of the 3rd layer faces the cold atmosphere to increase the temperature gradient. For the thermal balance estimation of ATE strips as shown Figure 9, we considered the following balance equation:

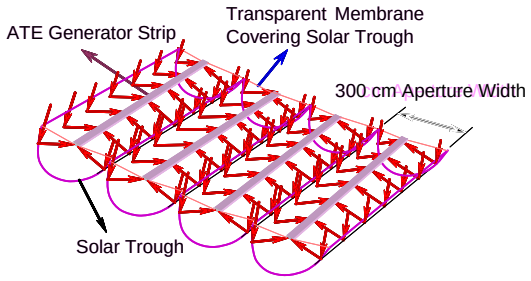

Figure 8. Solar trough with 300-cm aperture collects solar flux for ATE strip on each row.

$$\dot{q} = h_a(T_s - T_{air}) + \varepsilon_s \sigma (T_s^4 - T_{space}^4) \qquad (1)$$

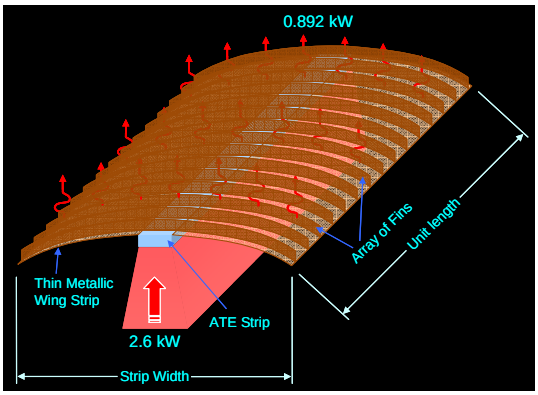

Figure 9. Extended cooling area by array of fins for radiative and convective losses.

where h_a is the heat transfer coefficient, W/m^2·°C, T_s the ATE strip surface temperature °C, T_{air} the air temperature (-73°C), σ the Steffan-Boltzmann constant, 5.6688 x 10^{-8} W/m^2·K^4, and ε_s the emissitvity of ATE surface. Assuming that the air at – 73 °C flows over the ATE strips with a uniform velocity and the ATE surface is maintained at a uniform temperature of 100 °C, the heat transfer coefficient h_a is determined by the Pohlhausen's solution [14]

$$h_a = 0.332\kappa_a \sqrt{\frac{V_a}{\upsilon_a L}}\,\mathrm{Pr}^{1/3} \qquad (2)$$

where κ_a is the thermal conductivity of air (≈ 0.02691 W/m·°C), V_a the air velocity, υ_a the kinematic viscosity of air (≈ 16.7 x 10^{-6} m^2/sec), L the width of ATE strip, and Pr the Prandtl number (≈ 0.711 for air). The Reynolds number of air flow (for V_a = 3 m/s) over the ATE strip amounts to

$$\mathrm{Re} = \frac{V_a \cdot L}{\upsilon_a} = \frac{3(m/s)\cdot 0.01(m)}{16.7x10^{-6}(m^2/s)} = 1796 \le \mathrm{Re}_L\ (\approx 5 \times 10^5) \qquad (3)$$

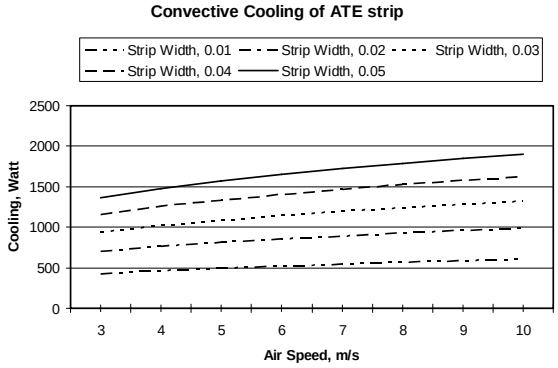

Figure 10. Cooling potential of various ATE strip size with fins with respect to air speed.

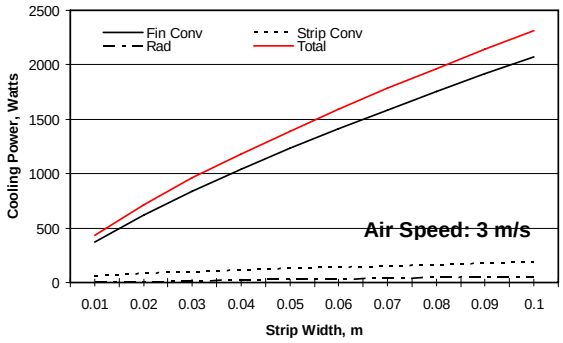

Figure 11. Cooling potential by fin, strip and radiative losses with respect to ATE strip size with fins at 3 m/s air speed.

The flow is considered laminar because $Re < Re_L$. The Peclet number (= Re·Pr) is 1277. Considering an array of 100 fins per meter attached on a cooling strip, the heat transfer rate for fins is defined by

$$q_f = e \cdot A_f \cdot h_f (T_s - T_a) \qquad (4)$$

where h_f is the heat transfer coefficient of fins which is determined by Eq. (4), A_f the area of fin, and e the fin efficiency which is determined by $e = \tanh(ml)/ml$ where $m = \sqrt{h_a / \kappa_a \cdot t_f}$. The t_f is the thickness of a fin. The total heat transfer rate of ATE strip is the summation of the heat losses by a strip and fins, as such $q_t = q_s + q_f$. Figures 10 and 11 show the cooling potential by the ambient air or by strip width with fins. Figure 10 shows the cooling potentials with respect to the air speed for the strip widths of 1 cm through 5 cm. In the case of a constant air speed (3 m/s), the cooling rate is dictated simply by the width of strip as shown in Figure 11. The solar energy collected by a 3-meter trough is approximately 4 kW. After the conversion process by the ATE, the power to be removed at the back surface of the ATE strip (i.e. 0.65Q-0.427Q) is 0.892 kW. In order to remove this amount of heat, the strip panel width for convective and radiative losses must be at least 0.03 meter or greater as shown in Figure 11. The extended metal strip is a thin-film structure with high emissivity and thermal conductivity to enhance the cooling of ATE strip.

The material for the reflector is an enhanced aluminum-coated thin-film membrane which is sufficiently hardened to maintain its parabolic shape. Each reflector is covered by a transparent membrane that allows sun light to impinge into the parabolic trough. The strip of ATE power module is located on a focal line of the parabolic trough and both edges of the strip are connected by the transparent thin-film window materials. The structural formation of such a solar trough should enhance the strength of the large-sized HAA.

II-5. Power Supply at Nighttime

The importance of nighttime power requirements may not be minimized because it has the same importance as daytime operation. Therefore, the power for the nighttime operation must be the same level as the daytime usage. Based on the daytime figure of power requirement, three components of the power infrastructure are actively involved to supply necessary power. For night time, the power required may be supplied from onboard fuel cells, batteries, and a rectenna array that is attached at the bottom surface of the HAA. These combined systems provide at least one megawatt level of power for intermittent operation.

Hydrogen fuel-cells with the capacity of at least a megawatt level are onboard for nighttime power generation. If we consider the power density of 500 W/kg, the fuel cell weighs two tons. The water which is an end product of fuel-cell process is collected and dissociated into hydrogen and oxygen through electrolysis process using the power harvested during daytime. The hydrogen and oxygen are collected and fed back to the fuel cells later at nighttime.

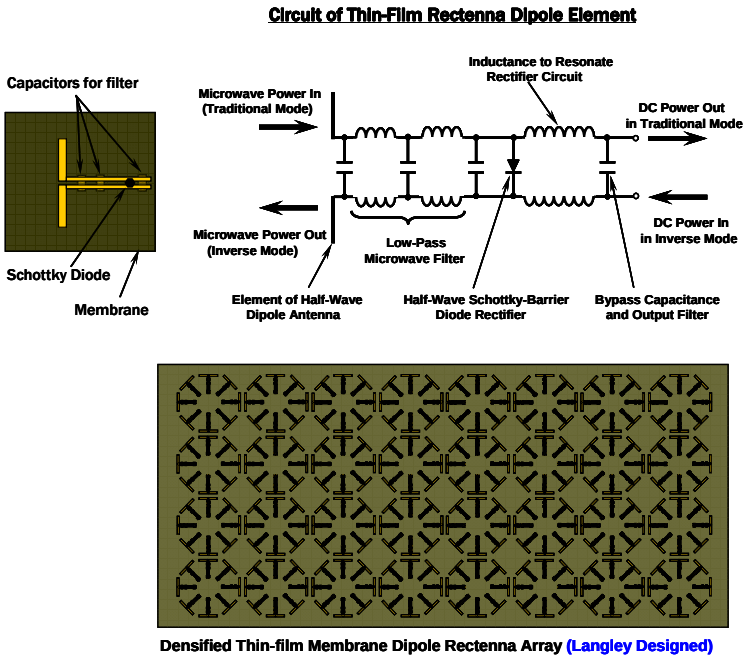

Figure 12. Dipole rectenna array on thin-film membrane.

The power stored in the thin-film battery during the day can be drained out for nighttime use. The battery storage capacity (~ 600 Coulomb/gram) is proportional to its own weight increase. Consequently, the battery is not regarded as the major power provider for nighttime use but can be used for emergency purposes.

The arrays of thin-film rectennas, as shown in Figure 12, can be readily fabricated on a flexible film which can be used as an integral part of balloon material for the bottom surface area of HAA. The arrays are patched under the bottom surface of HAA to receive and convert microwave power into DC Power. The conversion efficiency of rectenna is unusually high (~85%) [15-16], but the collection efficiency is poor because of the dispersive nature of microwaves. The bottom surface area of HAA is so wide and nearly flat that it is suitable to collect most of dispersed microwave. At the 21 km (~70,000 ft) altitude, the area required to collect the W-band (90~100 GHz) microwave is 48 meters in diameter. This number is calculated by the Gaubau relationship which is defined by the following formula:

$$\tau = \frac{\sqrt{A_r \cdot A_t}}{\lambda Z} \qquad (5)$$

where $\boldsymbol{A_r}$ is the area of receiving antenna, $\boldsymbol{A_t}$ the area of transmitting antenna, $\boldsymbol{Z}$ the distance between the transmitting and receiving antennas, λ the wavelength of microwave, and τ a parameter determined for 100% reception case of microwave energy, which is a value of 3.

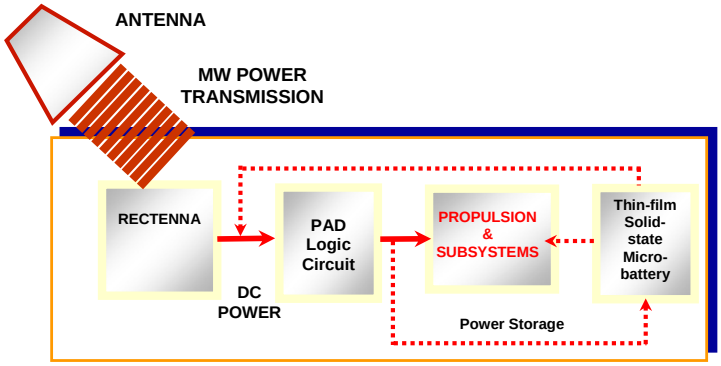

Figure 13. Logic diagram of microwave power use.

The bottom surface of HAA is 150 meters long and 60 meters wide. Accordingly, the microwave power at the W-band can be delivered to the array of rectennas at the bottom surface of HAA without significant losses. Figure 13 shows a logic diagram of the microwave power use. The power received by rectenna arrays is allocated and distributed by the power allocation and distribution (PAD) logic circuit to specific nodal points where the power is specifically required, such as propulsion units or subsystems. Otherwise, the excessive power is stored in an array of thin-film solid-state batteries for later use. Thus, a large amount of microwave power greater than a megawatt level can be delivered to the HAA from a ground or a ship-board microwave power beaming station in a controlled and safe manner over the prescribed distance. Even for a remotely dispatched HAA, wireless airborne electro-refueling by airplanes is possible. Multiple microwave stations combined can aim their beams onto a HAA to feed the power required for the operation at night.

III. Power Distribution and Uses

The power harvested by the ATE generator can be utilized for power transmission to microwave-powered aerial vehicles (MPAVs), for recharging on-board energy storage systems for night operation of the propulsion system, and for the internal power requirements such as propulsion and control. Figure 6 shows the graphical scenario of the HAA operational mode. If more power is required, it will need to build a larger HAA. The total power harvested (3.84 MW) is distributed for propulsion for stationary positioning and maneuvering, power storage, microwave beaming for MPAV operations, and house-keeping activities. Such applications require a continuous power source that will run for several hours in a sequential or a pulse mode anytime throughout the day and the night. Figure 14 shows the power flow diagram based on the power estimation that is to be harvested by the ATE array placed on top of the HAA. The power allocated for the operations of those onboard devices is purely estimated to give a glimpse at the power picture. In practice, a detailed study will be further required to determine the power demand of each application area. In this section, the power requirement of each segment is only guessed, but the accurate power requirements remain for further study.

III-1. Propulsion of HAA

The wind at an altitude of 21 km (70,000 feet) or above is substantially lower than typical seasonal jet-streams that exist within the northern hemisphere. Nevertheless, the large cross-sectional HAA needs significant power for propulsion, stability and control. Continuous positioning and maneuvering operations of the HAA against the wind is necessary and crucial for stationary operations and maximum solar exposure over solar angle variations. Otherwise, the HAA will drift away to a less desirable location where the use of onboard devices is not feasible. Propulsion for position correction and maneuvering is also required during the night time. Accordingly, a megawatt of power is allocated to sustain the necessary operation of HAA at day and night.

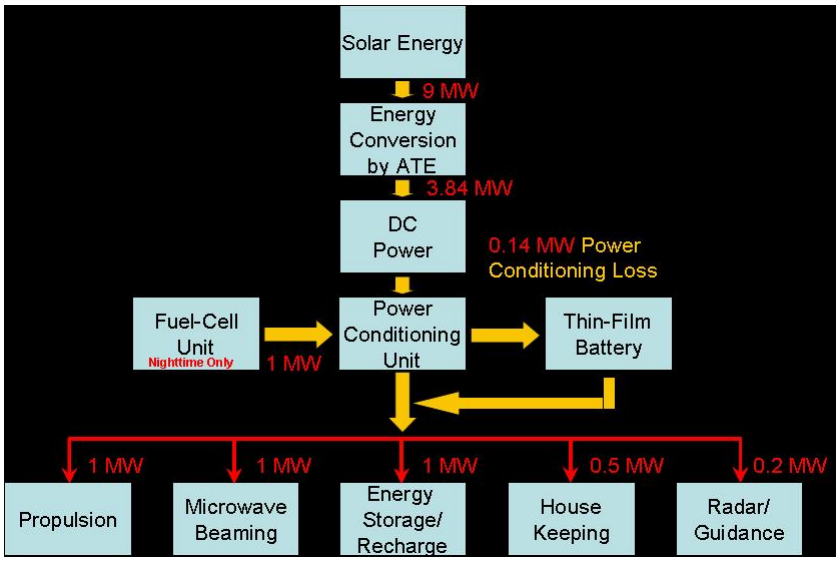

Figure 14. Power distribution scenario of the HAA for various onboard conceptual application devices.

III-2. Microwave Power Beaming for Helium-filled Aerial Vehicles

Microwave-Powered Aerial Vehicles (MPAV): A novel lightweight, high performance multifunctional structure is being developed for a long endurance microwave-powered aerial vehicle (MPAV) configuration that combines a polymer structure with an electrical power generating system to produce new missions and capabilities for air vehicles. As presently envisioned, this class of MPAVs satisfies NASA aeronautical missions for high altitude, characterized by long endurance, electric propulsion, propellantless, and emissionless. The configuration as conceived utilizes a polyimide structural material for creating the primary wing and fuselage elements of the vehicle. The polymer structure functions to carry normal, bending, and pressure loads as experienced from sea-level to cruising altitudes. The size of MPAV may be determined by its designated mission. The wing-span size of MPAV contemplated in this study is approximately 5 meters wide. The polymer structure incorporates the arrays of rectennas for wireless power generation system [17-18] in or around the dielectric layer of the power generating system as shown in Figure 15. The rectenna system has been demonstrated at microwave wavelengths (X-Band) to provide 275 volts from 18 milli-Watts of incident energy [19-20]. The rectenna system can be designed for other and higher frequencies depending on configuration requirements, atmospheric transmissibility, etc. The resulting electrical energy is intended for utilization as power for electrical motors for propulsion of the MPAVs alone, in combination with electrical storage systems, or in combination with other hydrocarbon engines, including hybrid modes of operation.

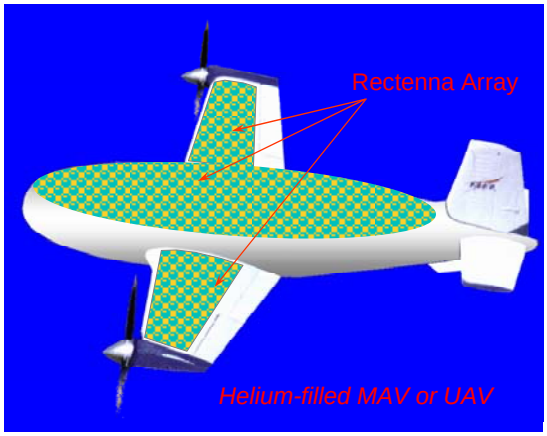

Figure 15. Helium-filled MPAV with electric propulsion. Wireless transmitted power is received by thin-film rectenna

As conceived, the MPAV is air-launched from and returned to the HAA base. The HAA based hangar for MPAVs is built under the HAA. The MPAVs are also launched or retrieved by hand, machine, towing, or dropped from other aircraft and / or helicopters. By nature of the structural material and concept of utilization,

the MPAV does not incorporate landing gear or skids. As such, the structural design requirements for takeoff, landing, and taxiing are reduced or eliminated and thereby relax the overall structural design loads and requirements.

For sustained long duration operations, a helium or helium/hydrogen mixture filled fat-body airframe for the MPAVs is proposed to reduce the power requirement for propulsion by both reducing the body weight and increasing the lift force by buoyancy. The fat-body framed MPAV model to be propelled by electric motors is shown in Figure 15. Two electric motor driven propellers are located at both the wing-tips and control the flight direction by changing rotational speed. The power for these planes is obtained from microwave transmission to rectenna arrays that are integrated on the skin of the airframe as shown in Figure 15. The range of maneuvers is determined by the envelope of the microwave beaming column and the guided direction of beam. As long as any MPAVs are within the beam column, the power is continuously fed into them. Suppose that a MPAV has a 10 m^2 rectenna array that is integrated into the skin of fuselage and both wings as shown Figure 15. If 1 MW of microwave power as described in the block diagram of Figure 14 is transmitted at W-band, the power flux density of microwave at the ground level is approximately 60 mW/cm^2. The power received by a MPAV which is a 20 km away to the ground level and has a 10 m^2 rectenna arrays will amount to be 6 kW within the power beam column of 50 meters in diameter. Using the same logic shown in Figure 13, the power is allocated to the propulsion system and other functional systems, such as probes. Suppose that the maneuver of the MPAV requires 4 kW of the received power. The rest can be used for sensors and probes for surveillance or for other operations. However, the power receiving area of MPAVs is limited due to their own limited sizes. Therefore, they need an extra lifting force to stay aloft. The helium-filled MPAVs as shown in Figure 14 will gain an extra lifting force. A helium-filled MPAV size of 5 m^3 will gain a buoyancy force of 51 N which will reduce the overall weight by 5 kg.

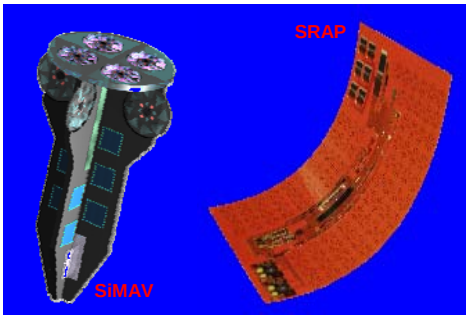

Figure 16. Free-flying sensors: a silicon-based micro aerial vehicle (SiMAV) [20] and sensor-rectenna array paper (SRAP) [21]

Figure 17. MPAV operation that drops off SiMAVs clustered with sensors.

Microwave-Powered Free Flying Sensors: The MPAV can be illustrated by both self-serving activities and mother-ship roles. A long duration flight of MPAV enables a sustained sensing and probing roles over long time without any interruption on a critical spot where the scientific assay is necessary. Although the flight speed of MPAV is slow in reality but due to its stability and duration it is more relevant to the temporal than spatial coverage. The self-serving roles of MPAV will require more power for sensor, probe, and telemetry systems than the power required for electric propulsion. As estimated earlier, a 6 kW of wirelessly transmitted power at W-band from the HAA suffices the needs for MPAV propulsion (4 kW) and a sensor cluster with telemetry system (2 kW). If any missions of MPAV require more power, a new design of MPAV will be necessary to accommodate the increases size of rectenna array. Otherwise, the operation range of MPAV must be closer to the HAA's beaming station to

Figure 18. Free-flying SRAP is deployed by MPAV over a volcano.

receive higher flux density of microwave than the reception at 20 km away.

As shown in Figure 16, the MPAV even carries free-flying sensors (FFS), such as a silicon-based micro aerial vehicle (SiMAV) [21] and sensor-rectenna array paper (SRAP) [22], to drop off to the location where critical data must be collected. The FFS can be dropped off from the MPAV sparsely over a wide area or densely on a spot. This type of operation reduces the power requirement of MPAV, since the FFS has their own power generators, such as micro-turbine with a capacitive power storage and imbedded rectenna array. The fabrication cost of FFS is very low, remaining under tens of dollars due largely to a large production yield of FFS under a conventional batch process by micro-fabrication. Accordingly, it would not be a significant issue for the FFS to be utilized once after deployment because of its abundance and low cost.

Figure 17 shows the deployment of SiMAV from a MPAV. The SiMAV has its own power generator based on an array of micro-turbines that use air flow to rotate the generator during the free flying period. The SiMAV has dual roles to collect the data during its flight or on the ground after soft landing. The excessive power generated by an array of micro-turbines will be stored into a capacitor which is built in the structure of SiMAV and will be used for sensing and probing on the ground after soft landing.

Figure 18 shows the free-flying SRAPs deployed from a MPAV. Interestingly, the SRAP does not require any onboard power generator, but simply takes microwave power which already exists to operate the MPAVs and converts it into DC power to run sensors clustered on SRAP. After soft landing, the SRAP can still execute its functions using microwave or power stored into the onboard thin-film capacitor.

III-3. Energy Storage/Recharge

The excessive energy harvested during the day time can be stored on onboard battery system, used to produce hydrogen by the breakdown of water molecules collected from fuel cell operation, or used for other utilities. Most of the Lidar systems for monitoring atmospheric constituent gases or pollutants require substantial power to operate. A Lidar system onboard the HAA can utilize the excessive power for its environmental monitoring operation, or the excessive power can be wirelessly transmitted to a remote area, such as deserts or Antarctic bases, where electricity is not readily available. Microwave rectenna array or laser can be used for wireless power transmission. NASA also developed new technologies and components for both microwave and laser power transmissions for space applications in the 1970s thru the 1980s. These technologies can be found from published articles, i.e. the rectenna array for microwave power transmission [8-13, 15], the directly solar pumped iodine laser and a high power diode laser array [23-25].

III-4. Power for House-Keeping

The internal power requirement is determined from the power consumption by the PMC station move over the guide rail, communication equipment, avionics, and system monitoring devices.

III-5. Power for Radar/Guidance

The onboard radar operation is necessary for monitoring other aircraft and air traffic control and management. The area of coverage provided by the 21 km cruise altitude is in excess of 300 nmi thereby allowing one airship to control an extensive amount of airspace.

IV. Configuration of HAA for Power Harvesting

The new concept airship has an elliptical cross-section perpendicular to the thrust axis to expand the solar exposure area unlike the conventional airships with a circular cross-section. The inset within Figure 6 shows the elliptical cross section of the airship. Accordingly, the overall shape of the new concept airship is a flattened elliptical cross-section as illustrated in Figure 6. Although the elliptical cross-section of the airship may be structurally less sturdy or slightly heavier than the circular cross-section, the benefits of the elliptical shape are greater considering the lift force and the stability of flight that might compensate the shortcomings of elliptical cross-section. If the structural reinforcement of the elliptical cross section should be required to maintain the same strength level of a circular cross sectioned, the weight increase due to the elliptical cross section of airship would be less than 20%. The near flat-top surface of the airship offers a wide area to accommodate a new

energy harvesting device from sun light, such as solar cells or advanced thermoelectric generators. The HAA has a guide rail to place the PMC station and the MPAV hangars to the nadir position of HAA. The purpose of rotational capability along the guide rail is to maximize the incidence of solar flux by setting the top surface of HAA always perpendicular to sun light. Whenever the PMC station moves on the guide rail, the HAA rotates and sets the PMC unit at the lowest level as shown in Figure 7 since the PMC station is the heaviest component of the HAA.

V. Summary

A new concept of High Altitude Airship configuration has been developed that utilizes a novel high-efficiency thermoelectric material being developed at the NASA Langley Research Center. Based on our theoretical estimation, the elliptical cross-section HAA concept with a tandem mode ATE energy harvesting system provides significant levels of power for various airship missions and applications. This exploratory system study has identified new missions and capabilities as well as benefits from utilizing advanced thermoelectric materials and devices for energy conversion. Many aspects of potential configuration and integration challenges for HAAs are not addressed, but a new shape of HAA for energy harvesting and few applications were somewhat generally elaborated in this configuration study.

References

[1] **http://www.nasa.gov/centers/dryden/news/FactSheets/FS-034-DFRC.html**

[2] L. Dubios et al., International Conference on Thermoelectrics (ICT-99).

[3] Sang H. Choi, Yeonjoon Park, Sang-Hyon Chu, James Elliott, Glen King, Jae-Woo Kim, Peter T. Lillehei, and Diane Stoakley, "Advanced Thermo-Electric Materials with Nano-Voids", Invention Disclosure, NASA Case No. LAR 16845-1, November 25, 2003.

[4] Yeonjoon Park, Sang H. Choi, and Glen C. King, "Lattice Matched SiGe Layer on Single Crystalline Sapphire Substrate", Invention Disclosure, NASA Case No. LAR 16868-1, February 26, 2004.

[5] Sang-Hyon Chu, Sang H. Choi, Jae-Woo Kim, Yeonjoon Park, James Elliott, Glen C. King, Diane M. Stoakley, "Fabrication of Nanovoid-imbedded Bismuth Telluride with Low Dimensional System", Invention Disclosure, NASA Case No. LAR 16906-1, April 13, 2004.

[6] Sang-Hyon Chu, Sang H. Choi, Jae-Woo Kim, Yeonjoon Park, James Elliott, Glen C. King, Diane M. Stoakley, "Fabrication of Advanced Thermoelectric Materials by Hierarchical Nanovoid Generation", Invention Disclosure, NASA Case No. LAR 16920-1, June 2, 2004.

[7] Jae-Woo Kim, Sang H. Choi, Peter T. Lillehei, Sang-Hyon Chu, Yeonjoon Park, Glen C. King, and James R. Elliott, "Fabrication of Metallic Hollow Nanoparticles", Invention Disclosure, Tracking ID 5018248, NASA Case No. LAR 17134-1, November 8, 2004.

[8] Jae-Woo Kim, Sang H. Choi, Peter T. Lillehei, Sang-Hyon Chu, Yeonjoon Park, Glen C. King, and James R. Elliott, "Fabrication of Metal Nanoshells Derived by a Biotemplate", Invention Disclosure, Tracking ID 5018379, NASA Case No. LAR 17135-1, December 28, 2004.

[9] Slack G. A. and M. A. Hussain, "The maximum possible conversion efficiency of silicon-germanium thermoelectric generators", J. of Appl. Phys. 70, pp2694-2718, 1 September 1991.

[10] **http://www.its.caltech.edu/~jsnyder/thermoelectrics/index.htm**.

[11] Purdue University Airship**, www.RenewableEnergyAccess.com**

[12] Private Communication with Chris Caylor, Research Triangle Institute Int'l, who just built a tandem TE system with conventional TE materials. February, 2006.

[13] Pathfinder Solar Plane flight records: **http://www.skytowerglobal.com/news-archive/news-pthfdr-2ndrecord/news-pthfdrtext.html**

[14] Latif M. Jiji, ***Heat Transfer Essentials: A Textbook***, Begel House Publishers, ISBN 1567001149, p7-19, 1998.

[15] Sang H. Choi, Kyo D. Song, Walter Golembiewskii, Sang-Hyon Chu, and Glen C. King: "Microwave Power for Smart Material Actuators", IOP Journal of Smart Materials and Structures, Vol. 13, No. 1, pp38-48, February 2004.

[16] Brown W.C. ***Rectenna technology program:*** "Ultralight 2.45GHz rectenna and 20GHz rectenna", NASA Contract Report CR179558 (Raytheon Report PT-6902), 1987.

[17] Sang H. Choi, Mark S. Lake, and Christopher Moore, "Microwave-driven Smart Material Actuators," Invention Disclosure, NASA Case No. LAR 15754-1, Sep. 24, 1998.

[18] Sang H. Choi, Walter T. Golembiewski, and Kyo D. Song, "Networked Array Circuitry for Power Allocation and Distribution (PAD)", Invention Disclosure, NASA Case No. LAR-16136-1-CU, July 31, 2000.

[19] Kyo D. Song, Won J. Yi, Sang-Hyon Chu and Sang H. Choi: "Microwave Driven Thunder Materials" Microwave and Optical Technology Letters, Vol. 36, No. 5, pp331-333, March 5, 2003.

[20] Kyo D. Song, Sang H. Choi, Walter T. Golembiewski, and Glen C. King: "Rectenna Performance under a 200 W Amplifier Microwave", Proceedings of SPIE, Smart Electronics, MEMS and Nanotechnology, Vol. 5389, Paper-06, pp26-33, March 15-18, 2004.

[21] Yeonjoon Park, Sang H. Choi, Glen C. King, and James R. Elliott, "Micro-Turbines and Micro-Coil Inductors for Electric Power Generation from Wind", Invention Disclosure, NASA Case No. LAR 17232-1, September 16, 2005.

[22] Sang H. Choi, Glen C. King, Yeonjoon Park, and James R. Elliott, "Free-Flying Sensor-Rectenna Array Paper (SRAP)", NASA Case No. LAR 17279-1, November 25, 2005

[23] Choi, S. H.; Lee, J. H.; Meador, W. E.; and Conway, E. J.: "A 50-kW Module Power Station of Directly Solar Pumped Iodine Laser," Journal of Solar Energy Engineering, ASME, Vol. 119, p.304, Nov. 1995.

[24] Choi, S. H., M. D. Williams, J. H. Lee, and E. J. Conway: ``Diode Laser Power Module for Beamed Power Transmission," Proceedings of the 26th IECEC, Boston, MA, Aug. 4-9, 1991.

[25] Choi, S. H., W. E. Meador, and J. H. Lee: ``Directly Solar-Pumped Iodine Laser for Beamed Power Transmission in Space," Proceedings of the 27 IECEC, Vol. 2, paper 929438, p2-305, San Diego, CA. Aug. 3-7, 1992.